Sensors and Actuators B 243 (2017) 380–387

Contents lists available at ScienceDirect

Sensors and Actuators B: Chemical

journal homepage: www.elsevier.com/locate/snb

Highly conductive polythiophene films doped with chloroauric acid for dual-mode sensing of volatile organic amines and thiols

Dengke Zhao[a], Ligui Li[a,b,c,*], Wenhan Niu[a], Shaowei Chen[a,d,*]

[a] New Energy Research Institute, College of Environment and Energy, South China University of Technology, Guangzhou Higher Education Mega Center, Guangzhou 510006, China
[b] Guangdong Provincial Key Laboratory of Atmospheric Environment and Pollution Control, College of Environment and Energy, South China University of Technology, Guangzhou 510006, China
[c] Guangdong Provincial Engineering and Technology Research Center for Environmental Risk Prevention and Emergency Disposal, China
[d] Department of Chemistry and Biochemistry, University of California, 1156 High Street, Santa Cruz, CA 95064, United States

ARTICLE INFO

Article history:
Received 17 June 2016
Received in revised form
15 November 2016
Accepted 2 December 2016
Available online 5 December 2016

Keywords:
Conducting polymer
Doping
Chemoresistive sensing
Amine
Thiol

ABSTRACT

Highly conductive polythiophene films with electrical conductivity of 71.7 S/cm were prepared by using a facile solution-processing method with $HAuCl_4$ as a dopant. The density of free charge carriers for thus-prepared polythiophene films was estimated to be $4.48 \times 10^{21}/cm^3$. In addition, upon doping, the color of the polymer films changed significantly with the main absorption peaks bathochromically shifted from the visible to near-infrared region. Interestingly, the polythiophene films could be easily dedoped when exposed to organic amines and thiols. The dual variations of film color and electrical conductivity thus were exploited for the design and fabrication of a logic circuit, in combination with polythiophene films doped by electrochemical oxidation, for selective detection of volatile amines and thiols with a detection limit lower than 1 ppm. The results demonstrate the high potential of this solution-doping method in the preparation of highly conducting organic thin films for vapor sensing.

1. Introduction

Conjugated polymers have been used extensively in thin-film organic electronics and sensors largely because of their mechanical flexibility, ready processability, widespread availability, ease of functionalization, and the highly tunable electrical conductivity [1–8]. In thin-film conjugated polymer based chemoresistive sensors, the sensitivity is strongly influenced by the electrical conductivity of conjugated polymers in active layer [7–10]. Normally, the electrical conductivity of conjugated polymers may be readily manipulated by doping methods. Of this, electrochemical oxidation, in principle, may be employed to dope almost any conjugated polymers [11,12]. However, electrochemical doping is usually confined to thin films on limited electrode surfaces rather than the bulk because of the marked increase of electrical resistance in thick films, and hence it is generally difficult to mass-produce doped conjugated polymers by using this method. In contrast, chemical doping represents an effective alternative which has been commonly used to tailor the conductivity of conjugated polymers. In fact, iodine and other strong oxidants, such as AsF_5 and $LiClO_4$, have been used extensively as dopants to increase the electrical conductivity of conjugated organic molecules [13–16]. However, the volatile nature of iodine and the harmful, strong oxidative properties of AsF_5 and perchlorate have restricted their practical applications. Thus, mild acids have been exploited as alternative dopants to endow conjugated polymers with an acceptable conductivity, and in some cases, also as guiding templates during synthesis to tailor the processability of the final products. For instance, poly(4-styrenesulfonic acid) has been widely used as a soft guiding template and dopant in the synthesis of water-dispersible poly(3,4-ethylenedioxythiophene):polystyrene sulfonate (PEDOT:PSS) [17,18], polyaniline:polystyrene sulfonate (PANI:PSS) [19,20] and polypyrrole:polystyrene sulfonate (PPY:PSS) [21,22] composites, which can form conductive and smooth thin films for organic electronics. However, the presence of an insulating PSS layer on the surface of the conducting polymer domains strongly impedes charge transport within the films, leading to much lower conductivity than that of the pristine films.

* Corresponding authors at: New Energy Research Institute, College of Environment and Energy, South China University of Technology, Guangzhou Higher Education Mega Center, Guangzhou 510006, China.
E-mail addresses: esguili@scut.edu.cn (L. Li), shaowei@ucsc.edu (S. Chen).

http://dx.doi.org/10.1016/j.snb.2016.12.018
0925-4005/

To (partially) compensate for the loss of conductivity, careful pre/post deposition treatments are generally needed [23–25], which complicates the device fabrication process. In some other studies, high conductivity of organic molecules is realized by a facile surface doping method with the self-assembly of silanes [26–28]. However, when exposed to moisture or hydroxyl containing compounds, the silanes become hydrolyzed and the conductivity of the organic molecules diminishes markedly, which suggests that silane dopants may be used only in moisture-free environments, strongly restricting their applications. Therefore, it remains challenging and yet desired to develop facile and effective strategies for the preparation of conjugated polymers with nonvolatile, intrinsic high conductivity.

Chloroauric acid ($HAuCl_4$), an acid with a standard reduction potential of +1.50 V, can be used as a p-type dopant for most conjugated organic molecules, and as a precursor for preparing Au nanoparticles in a variety of conjugated molecules [29–32]. However, the studies on the doping effect of $HAuCl_4$ on the electric conductivity and the applications in sensing of harmful volatile organic compounds have been scarce, to the best of our knowledge.

Herein, we used poly(3-hexylthiophene) (P3HT) as an illustrating example to examine the doping effect of $HAuCl_4$ on the corresponding optical property, electric conductivity and crystalline phase evolution. Interestingly, the resulting $HAuCl_4$-doped P3HT films exhibited a marked color change and an abrupt increase of the electrical conductivity to 71.7 S/cm; and the films might be readily dedoped by exposure to volatile organic amines and thiols, in contrast to electrochemically doped P3HT films. Logic gate sensors were therefore fabricated by the combination of the $HAuCl_4$-doped and electrochemically doped P3HT films for selective and sensitive detection of volatile organic amines and thiols, two harmful vapors that can be found in the atmosphere.

2. Experimental section

2.1. Materials

P3HT (Mw 100 000 g/mol and regioregularity better than 98%) was purchased from Rieke Metals Inc. $HAuCl_4$ and *o*-xylene (anhydrous, 99%) were purchased from Sigma-Aldrich Co. Ltd. Fuming sulphuric acid, methylamine and ethanethiol were purchased from Beijing Chemical Reagents Co. Ltd, China. All these chemicals were used as received without further treatment.

2.2. Preparation of P3HT nanowires and $HAuCl_4$-doped P3HT films

P3HT nanowires were prepared by adopting a literature procedure [1]. Briefly, 2 mL of xylene was added into a 20 mL glass vial containing 10 mg of P3HT, and the mixture was stirred at 75 °C for 4 h to obtain a P3HT solution at a concentration of 5 mg/mL. The obtained P3HT solution was naturally cooled to room temperature and kept in the dark for 72 h to allow the self-assembly of P3HT molecules into crystalline nanowires (Fig. S1). P3HT thin films were then prepared by drop casting 50 μL of the P3HT nanowire suspension on a clean glass slide where solvents evaporated at room temperature. The obtained dried films were then dipped into a 1 mM $HAuCl_4$ solution for 30 s, washed with copious deionized water and finally dried in air.

2.3. Characterization

Transmission electron microscopic (TEM) measurements were conducted on a Tecnai G2-F20 equipped with an EDX detector at an accelerating voltage of 100 kV. X-ray photoelectron spectroscopic

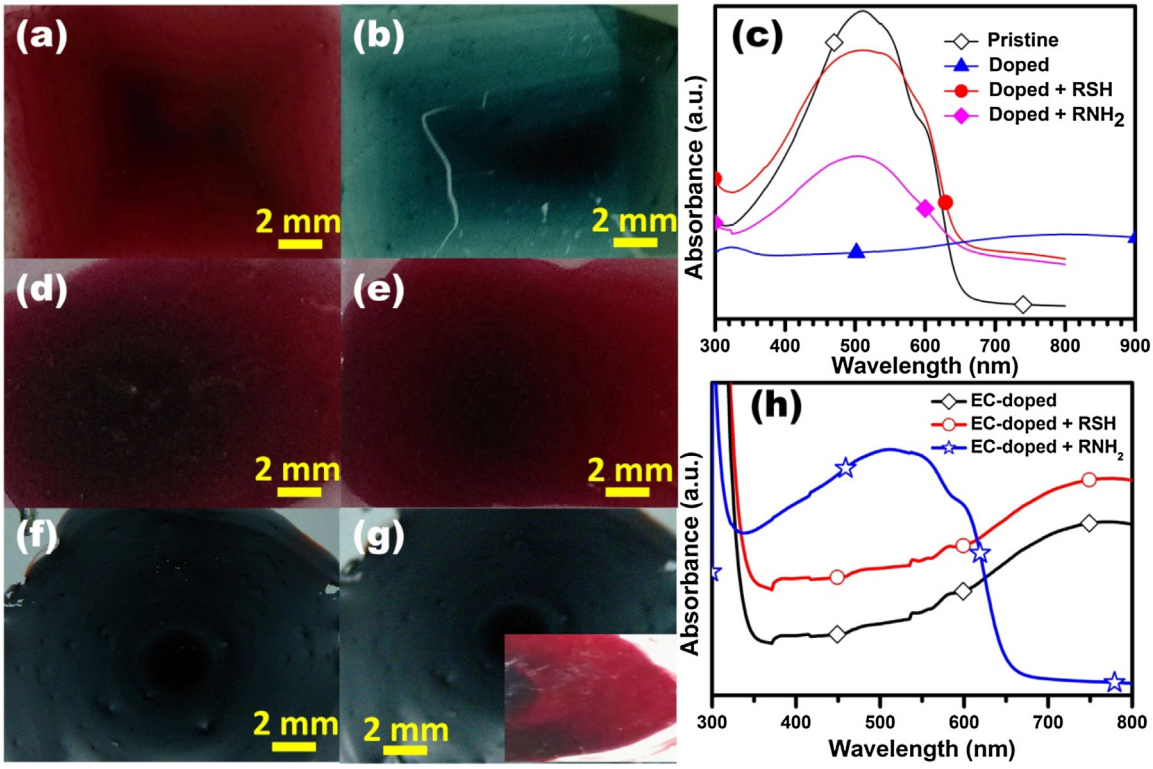

Fig. 1. (a, b, d–f, g) Optical images and (c, h) UV–vis absorption spectra of P3HT films after different treatments. (a) pristine, (b) doping by $HAuCl_4$ and subsequent exposure to 500 ppm of (d) CH_3NH_2 and (e) CH_3CH_2SH vapors; (f) electrochemical oxidation and (g) subsequently exposure to 500 ppm of CH_3CH_2SH vapor (inset is the film after exposure to CH_3NH_2).

Table 1
Logic relationships between organic vapors and film colors in Fig. 1.

	$HAuCl_4$-doped P3HT film	EC-doped P3HT film
RNH_2	1	1
RSH	1	0

(XPS) measurements were performed on a Phi X-tool instrument. X-ray diffraction (XRD) patterns were recorded with a Bruker D8-Advance diffractometer using Cu Kα radiation.

2.4. Electrochemical measurements

Electrochemical oxidation of the P3HT films were performed with a CHI 750E electrochemical workstation (CH Instruments, Chenhua Co., Shanghai, China) in a conventional three-electrode cell, with a platinum foil as the counter electrode, an Ag/AgCl as the reference electrode, P3HT films coated on a platinum foil as the working electrode, and an acetonitrile solution of 0.1 M $NaClO_4$ as the electrolyte.

2.5. Electrical conductivity measurements

Electrical conductivity measurements of the thin films were conducted with a KEITHLEY 2636B SYSTEM Source Meter using a 2-probe method. The samples were fixed at the bottom of a sealed 20 mL vial with an inlet near the vial bottom and an outlet near the vial opening (Fig. S2). Different concentrations of vapor were obtained by diluting the saturated analyte vapor at room temperature with dried air, and then 200 mL of the diluted vapors were injected into the vial through the inlet and the conductivity of the polymer thin films was measured.

3. Results and discussion

Fig. 1 shows the color evolution of a P3HT film that underwent different treatments. When the pristine P3HT film was dipped into a dilute $HAuCl_4$ solution, its color changed rapidly from red brown (Fig. 1a) to light blue (Fig. 1b), which suggested that the P3HT films had been successfully doped by $HAuCl_4$ [26]. In UV–vis absorption spectrum, three characteristic absorption peaks were observed in the pristine film (Fig. 1c, black curve). The peak at 508 nm was attributed to intrachain π-π* transition of the P3HT main chains, while the absorption peak at 610 nm was derived from the interchain π–π transition and its appearance signified the formation of ordered aggregates with interchain π–π stacking [33–35]. As for the vibronic shoulder peak at ca. 558 nm, it was normally ascribed to the absorptions of extended conjugation resulting from the ordered packing of the P3HT backbones in crystalline solids [35,36]. After doping by $HAuCl_4$ (denoted as "Doped" in Fig. 1c, blue curve), the absorption peak at 508 nm disappeared, while a new broad absorption peak centered at ca. 800 nm emerged. The latter is due to the polaron structure [24,37] of the polythiophene main chains, where the polarons were delocalized along the conjugated backbone of P3HT, leading to high conductivity. Moreover, a weak absorption peak centered at ca. 324 nm was also observed in the $HAuCl_4$-doped sample. This absorption peak is likely due to the $AuCl_4^-$ anions, suggesting the incorporation of the $AuCl_4^-$ anions in the P3HT films.

The color of the $HAuCl_4$-doped films could be effectively recovered by exposing the films to the vapors of organic amines or thiols. In fact, after exposure to 500 ppm of CH_3NH_2 (panel d) or CH_3CH_2SH (panel e) vapors, the color of the doped film returned to red brown, while it remained light blue in other common organic vapors such as hexane, ethanol and tetrahydrofuran (Fig. S3). In UV–vis absorption measurements (Fig. 1c, red and magenta curves), two apparent changes were observed. One is the reemergence of the strong peak at 508 nm, and the other is the disappearance of the peak at ca. 324 nm. These observations suggest that the doped film can be selectively dedoped by amines or thiols. This unique characteristic may be exploited for sensitive detection of these two volatile organic compounds (vide infra).

Interestingly, for P3HT films that were doped by electrochemical oxidation (not by $HAuCl_4$) [38], marked differences were observed when the films were exposed to the same volatile organic vapors. As shown in Fig. 1f, the electrochemically oxidized P3HT films,

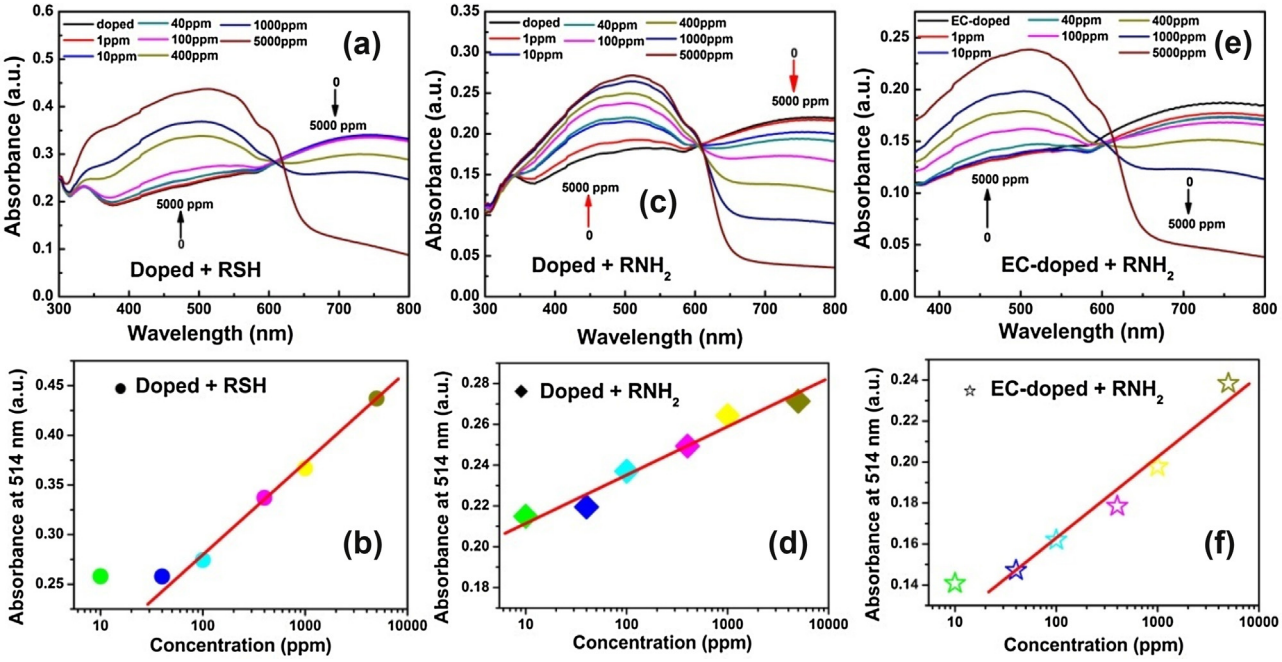

Fig. 2. (a, c, e) UV–vis absorption spectra of various P3HT films after exposure to different concentrations of organic vapors and (b, d, f) the dependence of absorbance at 514 nm on the vapor concentrations.

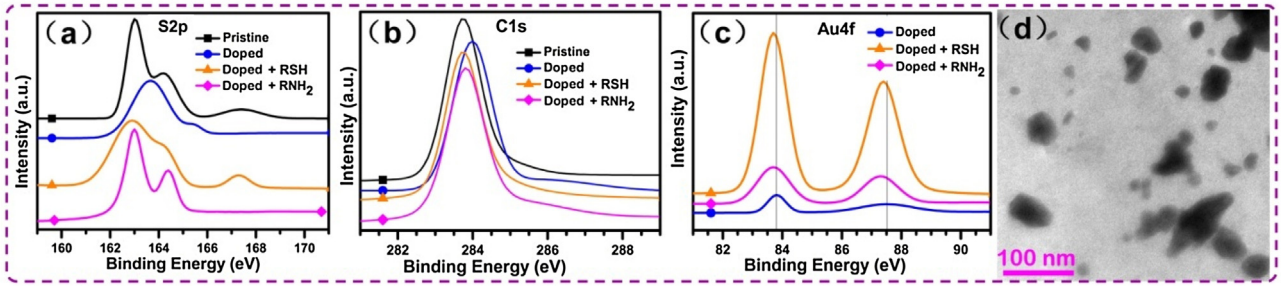

Fig. 3. High resolution XPS spectra of P3HT films with different treatments, (a) S2p electrons, (b) C1s electrons, (c) Au4f electrons. (d) TEM image of the $HAuCl_4$-doped P3HT film.

denoted as EC-doped, exhibited a dark blue color, and retained the blue color even after exposure to CH_3CH_2SH vapors (panel g); however, when exposed to the CH_3NH_2 vapor (inset to panel g), the dark blue film quickly changed back to red brown. Consistent results were observed in UV–vis absorption measurements. As depicted in Fig. 1h, the absorption spectra of the EC-doped film showed virtually no difference before and after exposure to CH_3CH_2SH vapors (black and red curves), featuring a broad peak at ca. 750 nm. In contrast, when the EC-doped film was exposed to 500 ppm of CH_3NH_2 vapors (blue curve), the absorption spectrum was almost identical to that of the pristine P3HT film (black curve).

On the basis of these results, if we use "1" and "0" to respectively denote the "red brown" and "blue" color of the P3HT films after exposure to organic vapors, a logic "AND" gate is formed for the selective detection of RSH and RNH_2 (Table 1).

The detailed evolution of the UV–vis absorption for the doped films was then studied as a function of the vapor concentrations. Fig. 2a depicts the UV–vis absorption spectra of $HAuCl_4$-doped film in the presence of CH_3CH_2SH vapors at various concentrations. One can see that with vapor concentration increasing from 1 ppm to 5000 ppm, the absorption intensity for the broad peak centered at ca. 750 nm gradually decreased. Concurrently, the absorption intensity at 508 nm, 558 nm and 610 nm steadily increased and finally recovered to that of pristine P3HT at 5000 ppm, where an isosbestic point at 610 nm was identified. Interestingly, the absorbance at 514 nm showed a linear dependent on the concentration of CH_3CH_2SH vapor in a wide range with a detection limit down to tens of ppm (Fig. 2b). When the doped film was exposed to CH_3NH_2, similarly evolution can be observed. After exposure to CH_3NH_2 vapors at as low as 1 ppm, the doped film was observed with a higher increment of the absorption intensity (Fig. 2c) than that in CH_3CH_2SH (Fig. 2a), which signified a higher detection limit for CH_3NH_2. Consistent results were observed in the linear dependence of absorbance at 514 nm on the CH_3NH_2 vapor concentration in a wider range from sub-ppm to thousands of ppm (Fig. 2d). In contrast, the EC-doped film demonstrated a detection limit of only a few tens ppm for CH_3NH_2 vapor (Fig. 2e, f). Taken together, these results show that doping P3HT thin films with $HAuCl_4$ enabled specific and sensitive colorimetric detection of volatile organic thiols.

The chemical structures of the $HAuCl_4$-doped P3HT films were then studied by XPS measurements. For the pristine P3HT sample (black curve), two strong peaks were observed at 163.0 eV and 164.2 eV, which were attributed to the S $2p_{3/2}$ and S $2p_{1/2}$ electrons, respectively. The broad peak centered at ca. 167.5 eV with a relatively low intensity is ascribed to R-SO_x moieties which are usually formed in polythiophenes because of partial oxidation of polythiophenes by H_2O and O_2 [39,40]. After doping by $HAuCl_4$ (blue curve), the binding energy of the S $2p_{3/2}$ and S $2p_{1/2}$ electrons shifted to higher values (163.6, 165.5 eV), suggesting that the sulfur atoms in P3HT backbones were oxidized by $HAuCl_4$ (vide infra). It is worthy to note that R-SO_x species were not observed in the doped films, probably because that the R-SO_x moieties were oxidized into small molecules and subsequently removed by water rinsing. Similar observations were observed in the C 1s spectrum. As shown in Fig. 3b, $HAuCl_4$ doping also caused a slight blue shift of the binding energy of the C 1s electrons from 283.8 eV to 284.0 eV (black and blue curves). From the XPS spectra of Au 4f electrons in Fig. 3c, one can observe two peaks at 83.8 eV and 87.5 eV, consistent with those of metallic gold [41]. This signifies the reduction of $HAuCl_4$ by P3HT. In fact, TEM measurements clearly showed the formation of gold nanoparticles in the films (Fig. 3d).

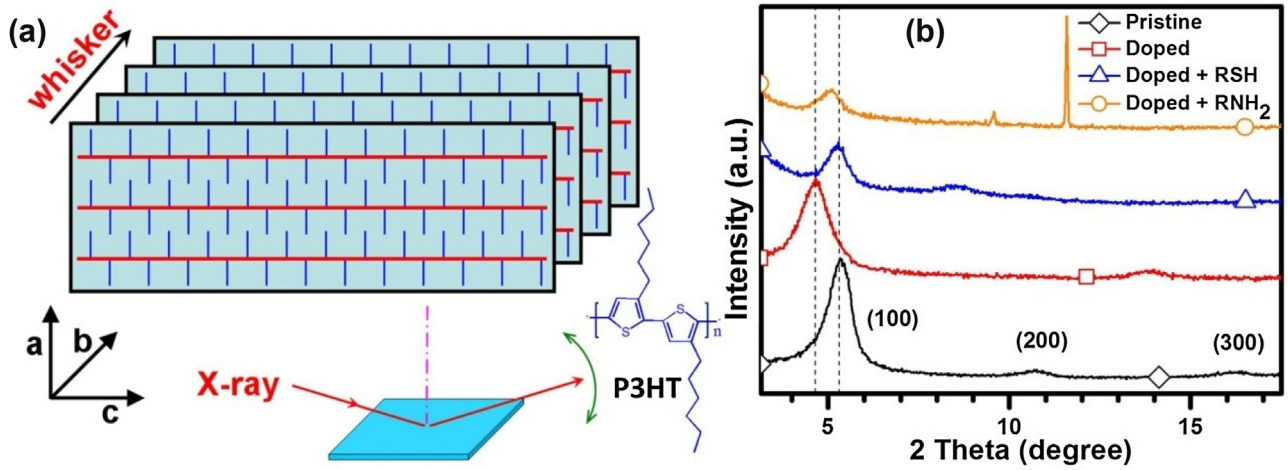

Fig. 4. (a) Schematic illustrating the working mode of XRD measurements and the crystallographic orientation of P3HT crystal. (b) XRD profiles of P3HT films after different treatments.

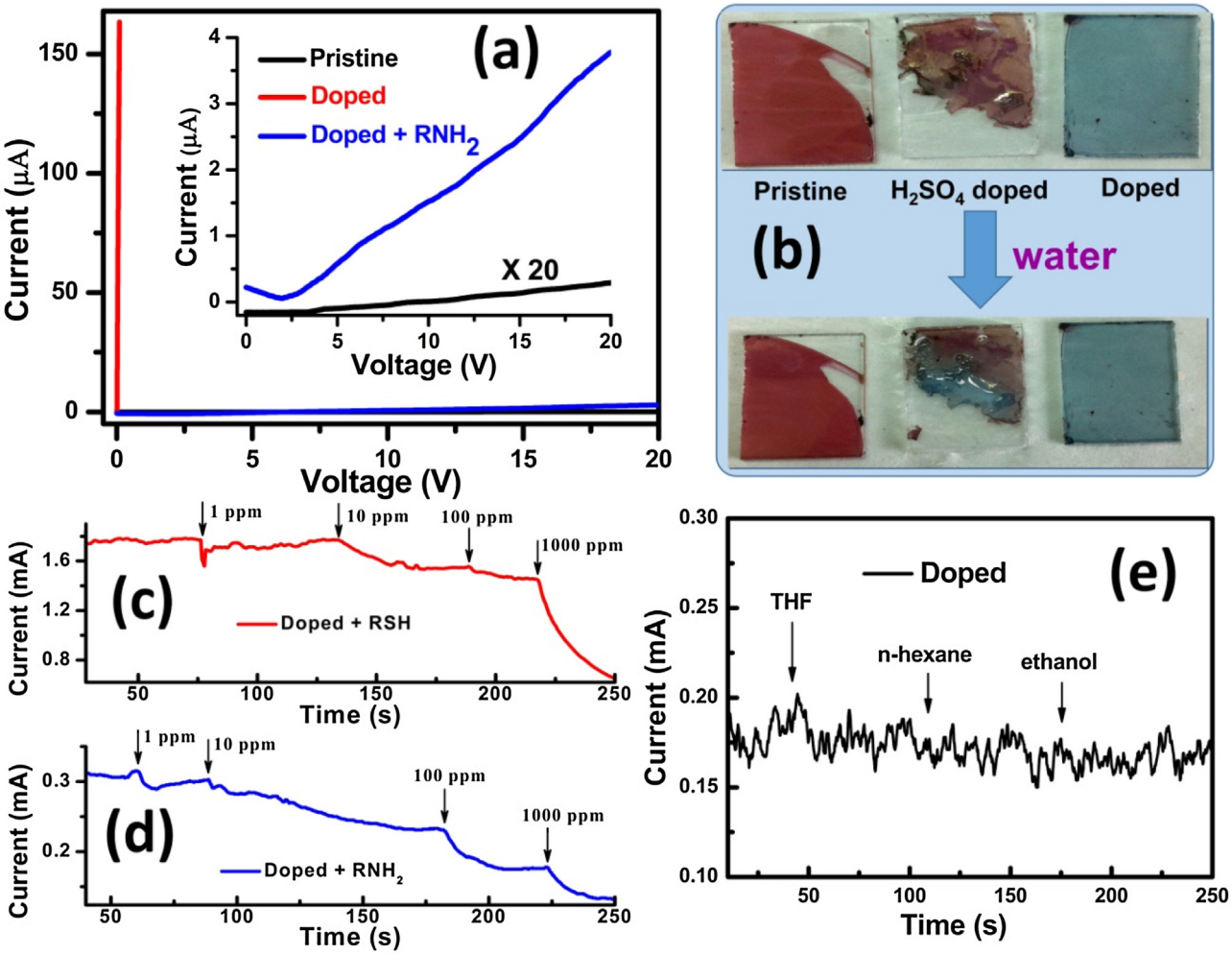

Fig. 5. (a) I–V curves of P3HT films after different treatments; inset is the zoom-in image showing the I–V curves of the pristine and doped + RNH_2 samples. (b) Photographs showing the stability of P3HT films at different doping states. Current-time plots of doped films at a constant bias voltage of 10 V and exposed to (c) CH_3CH_2SH and (d) CH_3NH_2 vapors at different concentrations. (e) Current-time plot of a doped film at a constant bias voltage of 10 V and exposed to 1000 ppm of THF, *n*-hexane and ethanol vapors.

When the doped films were exposed to volatile amines and thiols, dedoping of P3HT occurred, as evidenced by the recovery of the binding energies of the S 2p and C 1s electrons to those of pristine P3HT (Fig. 3a, b) and a red shift of 0.1–0.2 eV of the binding energy of the Au 4f electrons (Fig. 3c). One may note that when the $HAuCl_4$-doped films were exposed to CH_3CH_2SH vapors (orange curve), the S 2p electrons at 167.5 eV also appeared, while no such peak could be observed with the sample that was exposed to CH_3NH_2 (denoted as "doped + RNH_2") at the same binding energy. This observation further confirms that the peak of S 2p electrons at 167.5 eV observed in the pristine P3HT film is indeed due to the R-SO_x moiety because of partial oxidation of P3HT. Additionally, it suggests that CH_3CH_2SH was oxidized to R-SO_x by $AuCl_4^-$ leading to dedoping of the polymer thin films.

During the doping/dedoping process, the crystalline structure of P3HT also underwent substantial changes. In XRD measurements in the θ–2θ out-of-plane scanning mode (Fig. 4a), three pronounced diffraction peaks can be identified at $2\theta = 5.32°$, 10.71° and 16.13° in the pristine P3HT films (Fig. 4b), which may be ascribed to the diffractions of the (100), (200) and (300) planes with a d-spacing of 16.61 Å, 8.26 Å and 5.50 Å, respectively [35,42]. After doping by $HAuCl_4$, the (100) and (300) diffraction peaks shifted to lower angles of 4.63° and 13.89°, and the corresponding d-spacing increased to 19.10 Å and 6.38 Å, respectively. These values are much larger than those of the pristine P3HT. Such lattice expansion likely resulted from the intercalation of large counter anions of $AuCl_4^-$ in the crystal. The disappearance of the (200) diffraction peak in the doped sample was probably due to the change of the crystal symmetry after the inclusion of $AuCl_4^-$ anions in the lattices. When the doped film was exposed to CH_3CH_2SH, the 2θ angle of the (100) diffraction peak returned to that of pristine P3HT. Additionally, a new peak at $2\theta = 8.49°$ appeared, which might be ascribed to the diffraction of crystalline R-SO_x byproducts. In contrast, when the doped film was exposed to CH_3NH_2, the (100) diffraction peak was found at $2\theta = 5.09°$, corresponding to a d-spacing of 17.36 Å that was slightly larger than that of pristine P3HT. Moreover, two diffraction peaks at 2θ of 9.58° and 11.57° were also observed, which likely arose from crystalline amino salts derived from CH_3NH_2 and $HAuCl_4$.

The electrical conductivity of the P3HT films also varied with the doping states. As shown in Fig. 5a, even at a bias voltage of 20 V, the current of the pristine P3HT film was only in the order of nA (black curve), corresponding to low electric conductivity of ca. 47.2 μS/cm. However, after doping by $HAuCl_4$, the current increased markedly even at a very small bias voltage of 0.1 V (red curve), and the electrical conductivity was remarkably enhanced to 71.7 S/cm. It is worthy to note that the high electrical conductivity of $HAuCl_4$-doped P3HT is not due to the formation of gold nanoparticles but to the doped

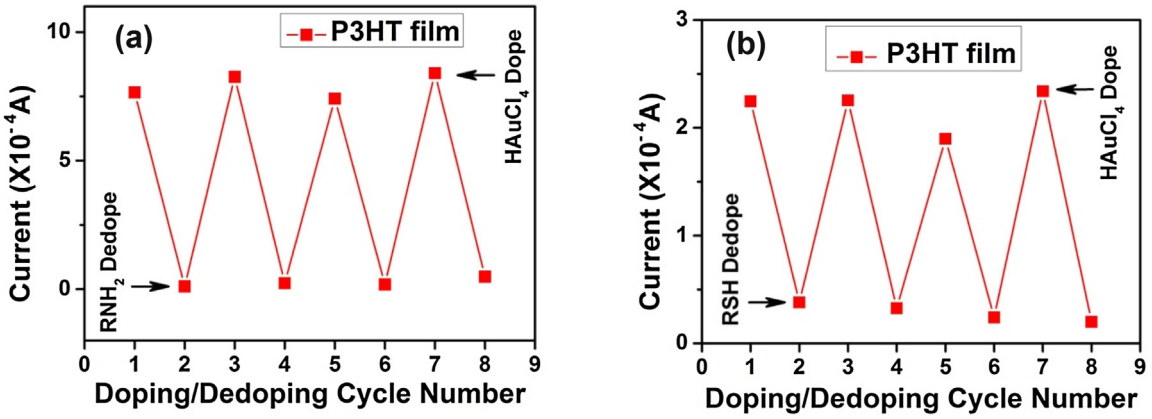

Fig. 6. The current evolution of P3HT films after different cycles of $HAuCl_4$ doping and dedoping with different volatile vapors at a concentration of 100 ppm under a constant voltage bias of 1 V. (a) CH_3NH_2 vapor; (b) CH_3CH_2SH vapor.

P3HT itself. This is supported by an abrupt decrease of the conductivity to 7.74 mS/cm when the $HAuCl_4$-doped P3HT film was exposed to 1000 ppm of CH_3NH_2 vapor (blue curve). Therefore, doping of P3HT with $HAuCl_4$ helped to generate a large number of free charge carriers in P3HT. The density of charge carriers (n_h) was evaluated to be $4.48 \times 10^{21}/cm^3$ by the following equation which correlates the electrical conductivity (σ = 71.7 S/cm for the doped P3HT) with mobility ($\mu \approx 0.1\ cm^2/V$ for a typical hole mobility of P3HT [2,27,42]), $\sigma = en_h\mu$, where e is the elementary charge. Such a high charge carrier density in $HAuCl_4$-doped P3HT is highly comparable to that induced by electrolyte gating [27,43]. Taking the density of P3HT (normally 1.1 g/cm^3) [44] into account, our calculation suggests that on average one hole was created on each 3-hexylthiophene repeating units after $HAuCl_4$ doping. Moreover, the conductivity of $HAuCl_4$-doped P3HT is nonvolatile as compared with that commonly observed with films doped by fuming H_2SO_4 in air. As shown in Fig. 5b, the light blue H_2SO_4-doped film gradually changed back to red brown within a few min in air, indicative of dedoping of P3HT due to the absorption of moisture from air. In contrast, the $HAuCl_4$-doped P3HT film retained its blue color even after extensive washing with distilled water. That is, a high doping level (approximately one hole per thiophene ring) and stable conducting state were achieved on P3HT films through this simple $HAuCl_4$ doping.

The conductivity of the $HAuCl_4$-doped P3HT films is sensitive to amines and thiols. As shown in Fig. 5c, d, the conductivity of the $HAuCl_4$-doped P3HT films decreases with increasing concentration of CH_3CH_2SH or CH_3NH_2 vapors, even down to 1 ppm. Such dedoping effects might be ascribed to the redox reactions as manifested in XPS measurements (Fig. 3), with minimal contributions from de-protonation of the polymer film [12,45]. In fact, when the P3HT film was subsequently exposed to HCl vapors after being dedoped by CH_3NH_2, the conductivity did not recover to that before exposure to CH_3NH_2 (Fig. S4). Notably, the $HAuCl_4$-doped films showed no response to other common organic solvent vapors such as tetrahydrofuran, *n*-hexane and ethanol (Figs. 5 e and Fig. S3), demonstrating the selective sensing of amines and thiols.

Moreover, the doping and dedoping process with $HAuCl_4$ and volatile organic amines/thiols, respectively, is highly reversible. As shown in Fig. S5 and Fig. 6, exposing the freshly prepared $HAuCl_4$-doped P3HT to 100 ppm volatile organic amines/thiols results in low electrical conductivity, but their high electrical conductivity can be recovered by redoping with $HAuCl_4$. After 4 cycles of doping/dedoping processes, the $HAuCl_4$-doped films can still sense CH_3NH_2 and CH_3CH_2SH vapor, which signify the high reversibility of present P3HT thin film-based sensors for volatile organic amines and thiols.

Taken together, the above results suggest that when P3HT film is doped by $HAuCl_4$, partial thiophene rings on P3HT chain are oxidized into R-SOx and small molecules, along with the formation of Au nanoparticles. Concurrently, partial thiophene rings may also form charge-transfer-like complex with $AuCl_4^-$ due to the strong bonding affinity between sulfur atom in thiophene ring and Au atom in $AuCl_4^-$[46,47], with partial electrons transferring from thiophene ring to Au atom in $AuCl_4^-$, which generate free hole charge carriers, i.e. polarons/bipolarons, and hence lead to a high electrical conductivity. Exposing the $HAuCl_4$-doped P3HT film to amines causes the loss of polarons/bipolarons due to the reduction of $AuCl_4^-$ by the reducing amines. In the case of exposure to thiols, thiols may compete with thiophene rings to bond with $AuCl_4^-$, which strongly weaken the interaction between thiophene ring and $AuCl_4^-$ and hence cause dedoping in P3HT film, resulting in low electrical conductivity. When P3HT film is doped by electrochemical oxidation, free hole charge carriers (i.e. polarons/bipolarons) are also generated on P3HT molecular chain, leading to a high electrical conductivity. Exposing the EC-doped P3HT film to amine vapors, the amines that show strong electron donating ability bind with cation-like thiophene rings and partially donate the lone electron pair of nitrogen in amine molecule to the cation-like thiophene ring, which significantly decreases the number of polarons/bipolarons on P3HT, resulting in low electrical conductivity. The dedoping process of EC-doped P3HT film with amines highly resembles the dedoping of acid-doped polyaniline with amines. In contrast, the electron donating ability of sulfur atom in thiols is not as strong as nitrogen atom in amines, therefore EC-doped P3HT film can retain its doped state after exposing to thiols.

The dependence of the electrical conductivity of P3HT on the doping state may be exploited for chemoresistive sensing of volatile amines and thiols. To ensure selectivity, two EC-doped films and two $HAuCl_4$-doped films were assembled into a device, as depicted in Fig. 7a, with the equivalent circuit shown in Fig. 7b. When the sensor is powered, both L1 (red) and L2 (blue) LED lights are on (the "on" state). When organic thiols present in the testing environment, the $HAuCl_4$-doped films (denoted as R_{doped}) are dedoped and the resistance of both R_{doped} increase by orders of magnitude while the two $R_{EC\text{-}doped}$ remained at low resistance. Consequently, the current through L1 was significantly reduced and hence L1 was turned off, leading to an "off" state for L1. In contrast, the current through L2 was only slightly decreased, remaining an "on" state for L2, as shown in Fig. 7c. Using "1" and "0" to respectively denote

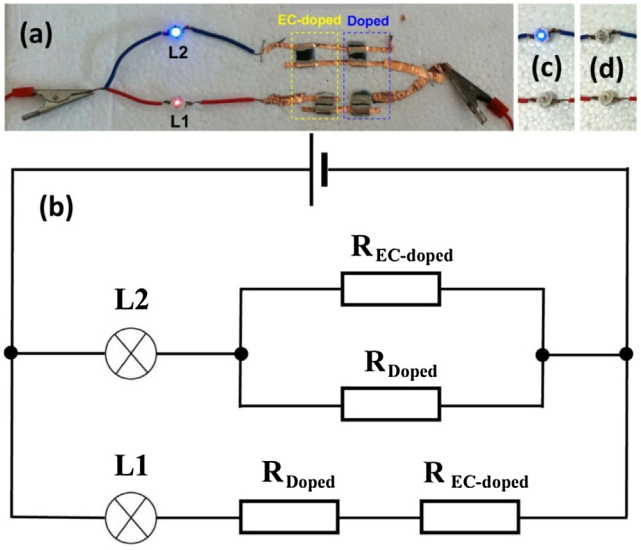

Fig. 7. (a) Photo image of a sensing device and (b) its equivalent circuit. (c, d) Photo images of the on/off states of the lights in (a) when the device is exposed to 50 ppm CH_3CH_2SH and CH_3NH_2 vapors, respectively. All measurements herein were conducted at a constant bias voltage of 10 V.

Table 2
Logic relationships between organic vapors and the on/off states of L1 and L2 LED lights in Fig. 6.

	L1	L2
RSH	0	1
RNH_2	0	0

the "on" and "off" states of the LED lights, the logic response of L1 and L2 in sensor device to thiol vapor was summarized in row 1 in Table 2. While in the presence of organic amines, the resistance of both the $R_{EC\text{-}doped}$ and R_{doped} increased by orders of magnitude, which caused drastic decrease of current through both L1 and L2 and hence both lights became off, leading to an "off" state for both L1 and L2 (Fig. 7d and Row 2 in Table 2). Therefore, one can see that the on/off states of L1 demonstrate if RNH_2 or RSH is present in the vapor, while the on/off states of L2 identify that the gas vapor is RSH or RNH_2. Based on the logic relations demonstrated in Table 2, a logic "OR" gate is formed for the sensitive detection of RSH and RNH_2.

Therefore, by utilizing the change of color/light absorption and conductivity associated with the doping/dedoping of P3HT, a dual-mode sensing of volatile organic amines and thiols was successfully achieved. Note that whereas the signal to noise ratio (S/N) and detection limit of volatile amines and thiols remains to be further enhanced, the fact that intrinsic high conductivity of conjugated polymer films can be directly obtained by a simple one-step doping procedure suggests that higher conductivity and lower detection limit might be realized by deliberate optimization of the doping conditions and selection of other conjugated polymers which have higher crystallization ability [27,48–50].

4. Conclusion

Doping of P3HT films by aqueous $HAuCl_4$ solution formed oxidized polymer backbones with $AuCl_4^-$ acting as the counter anions. This led to an apparent expansion of the crystalline lattices and marked variations of the optical and electronic properties of the polymer films, as manifested by a significant bathochromic shift of the absorption features, and enhanced conductivity resulting from the formation of a large number of free charge carriers. These doped films could be readily dedoped by exposure to organic amines or thiol vapors, in contrast to the electrochemically doped counterparts. The associated colorimetric and chemoresistive changes during the dedoping process enabled dual mode logic-gate sensing of these two volatile harmful vapors with high selectivity. These results highlight the potential of using this facile doping method for the preparation of highly conductive conjugated polymers for vapor sensing and organic electronics.

Author contributions

The manuscript was written through contributions of all authors. All authors have given approval to the final version of the manuscript.

Acknowledgments

This work was partially supported by the National Recruitment Program of Global Experts. L.G.L. acknowledges the financial support from the National Natural Science Foundation of China (NSFC)51402111) and the Scientific Research Foundation for the Returned Overseas Chinese Scholars, State Education Ministry. S.W.C. thanks the National Science Foundation (CHE-1265635 and DMR-1409396) for partial support of the work.

Appendix A. Supplementary data

Supplementary data associated with this article can be found, in the online version, at http://dx.doi.org/10.1016/j.snb.2016.12.018.

Schematic of experimental setup, TEM micrograph, photographs and additional data.

References

[1] Y. Huang, E.J. Kramer, A.J. Heeger, G.C. Bazan, Bulk heterojunction solar cells: morphology and performance relationships, Chem. Rev. 114 (2014) 7006–7043.
[2] R. Noriega, J. Rivnay, K. Vandewal, F.P.V. Koch, N. Stingelin, P. Smith, et al., A general relationship between disorder, aggregation and charge transport in conjugated polymers, Nat. Mater. 12 (2013) 1038–1044.
[3] H.-R. Tseng, H. Phan, C. Luo, M. Wang, L.A. Perez, S.N. Patel, et al., High-mobility field-effect transistors fabricated with macroscopic aligned semiconducting polymers, Adv. Mater. 26 (2014) 2993–2998.
[4] H. Zheng, Y. Zheng, N. Liu, N. Ai, Q. Wang, S. Wu, et al., All-solution processed polymer light-emitting diode displays, Nat. Commun. 4 (1971) (2013), http://dx.doi.org/10.1038/ncomms2971.
[5] M. He, F. Qiu, Z. Lin, Towards high-performance polymer-based thermoelectric materials, Energy Environ. Sci. 6 (2013) 1352–1361.
[6] L. Li, L.-H. Ferng, Y. Wei, C. Yang, H.-F. Ji, Highly stable polyaniline-poly(sodium 4-styrenesulfonate) nanoparticles for sensing of amines, J. Nanosci. Nanotechnol. 14 (2014) 6593–6598.
[7] C. Wang, B.R. Bunes, M. Xu, N. Wu, X. Yang, D.E. Gross, et al., Interfacial donor-acceptor nanofibril composites for selective alkane vapor detection, ACS Sens. 1 (2016) 552–559.
[8] Y. Zhang, M. Xu, B.R. Bunes, N. Wu, D.E. Gross, J.S. Moore, et al., Oligomer-coated carbon nanotube chemiresistive sensors for selective detection of nitroaromatic explosives, ACS Appl. Mater. Interfaces 7 (2015) 7471–7475.
[9] K. Low, C.B. Horner, C. Li, G. Ico, W. Bosze, N.V. Myung, et al., Composition-dependent sensing mechanism of electrospunconductive polymer composite nanofibers, Sens. Actuators B Chem. 207 (2015) 235–242.
[10] I. Fratoddi, I. Venditti, C. Cametti, M.V. Russo, Chemiresistive polyaniline-based gas sensors: a mini review, Sens. Actuators B Chem. 220 (2015) 534–548.
[11] E.W.H. Jager, E. Smela, O. Inganäs, Microfabricating conjugated polymer actuators, Science 290 (2000) 1540–1545.
[12] A.G. MacDiarmid, Synthetic metals: a novel role for organic polymers (Nobel lecture), Angew. Chem. Int. Ed. 40 (2001) 2581–2590.
[13] T.J. Prosa, M.J. Winokur, J. Moulton, P. Smith, A.J. Heeger, X-ray-diffraction studies of the three-dimensional structure within iodine-intercalated poly(3-octylthiophene), Phys. Rev. B 51 (1995) 159–168.
[14] C.K. Chiang, C.B. Fincher Jr., Y.W. Park, A.J. Heeger, H. Shirakawa, E.J. Louis, et al., Electrical conductivity in doped polyacetylene, Phys. Rev. Lett. 39 (1977) 1098–1101.

[15] T.-C. Chung, J.H. Kaufman, A.J. Heeger, F. Wudl, Charge storage in doped poly(thiophene): optical and electrochemical studies, Phys. Rev. B 30 (1984) 702–710.
[16] K. Tashiro, M. Kobayashi, T. Kawai, K. Yoshino, Crystal structural change in poly(3-alkyl thiophene)s induced by iodine doping as studied by an organized combination of X-ray diffraction, infrared/Raman spectroscopy and computer simulation techniques, Polymer 38 (1997) 2867–2879.
[17] F. Louwet, L. Groenendaal, J. Dhaen, J. Manca, J.V. Luppen, E. Verdonck, et al., PEDOT/PSS: synthesis, characterization, properties and applications, Synth. Met. 135–136 (2003) 115–117.
[18] L.B. Groenendaal, F. Jonas, D. Freitag, H. Pielartzik, J.R. Reynolds, Poly(3,4-ethylenedioxythiophene) and its derivatives: past, present, and future, Adv. Mater. 12 (2000) 481–494.
[19] W. Liu, J. Kumar, S. Tripathy, K.J. Senecal, L. Samuelson, Enzymatically synthesized conducting polyaniline, J. Am. Chem. Soc. 121 (1999) 71–78.
[20] L. Li, L. Ferng, Y. Wei, C. Yang, H.-F. Ji, Effects of acidity on the size of polyaniline-poly(sodium 4-styrenesulfonate) composite particles and the stability of corresponding colloids in water, J. Colloid Interface Sci. 381 (2012) 11–16.
[21] C.K. Baker, Y.J. Qiu, J.R. Reynolds, Electrochemically-induced charge and mass transport in polypyrrole/poly(styrene sulfonate) molecular composites, J. Phys. Chem. 95 (1991) 4446–4452.
[22] L.-X. Wang, X.-G. Li, Y.-L. Yang, Preparation, properties and applications of polypyrroles, React. Funct. Polym. 47 (2001) 125–139.
[23] Y.H. Kim, C. Sachse, M.L. Machala, C. May, L. Müller-Meskamp, K. Leo, Highly conductive PEDOT:PSS electrode with optimized solvent and thermal post-treatment for ITO-Free organic solar cells, Adv. Funct. Mater. 21 (2011) 1076–1081.
[24] J.E. Yoo, K.S. Lee, A. Garcia, J. Tarver, E.D. Gomez, K. Baldwin, et al., Directly patternable, highly conducting polymers for broad applications in organic electronics, Proc. Natl. Acad. Sci. 107 (2010) 5712–5717.
[25] J. Zhou, D.H. Anjum, G. Lubineau, E.Q. Li, S.T. Thoroddsen, Unraveling the order and disorder in poly(3, 4-ethylenedioxythiophene)/poly(styrenesulfonate) nanofilms, Macromolecules 48 (2015) 5688–5696.
[26] M.F. Calhoun, J. Sanchez, D. Olaya, M.E. Gershenson, V. Podzorov, Electronic functionalization of the surface of organic semiconductors with self-assembled monolayers, Nat. Mater. 7 (2008) 84–89.
[27] C.Y. Kao, B. Lee, L.S. Wielunski, M. Heeney, I. McCulloch, E. Garfunkel, et al., Doping of conjugated polythiophenes with alkyl silanes, Adv. Funct. Mater. 19 (2009) 1906–1911.
[28] H. Huang, D.E. Gross, X. Yang, J.S. Moore, L. Zang, One-step surface doping of organic nanofibers to achieve high dark conductivity and chemiresistor sensing of amines, ACS Appl. Mater. Interfaces 5 (2013) 7704–7708.
[29] J. Han, L. Li, R. Guo, Novel approach to controllable synthesis of gold nanoparticles supported on polyaniline nanofibers, Macromolecules 43 (2010) 10636–10644.
[30] X. Liu, L. Li, M. Ye, Y. Xue, S. Chen, Polyaniline:poly(sodium 4-styrenesulfonate)-stabilized gold nanoparticles as efficient, versatile catalysts, Nanoscale 6 (2014) 5223–5229.
[31] C.-H. Lai, I.-C. Wu, C.-C. Kang, J.-F. Lee, M.-L. Ho, P.-T. Chou, Homogeneous, surfactant-free gold nanoparticles encapsulated by polythiophene analogues, Chem. Commun. (2009) 1996–1998.
[32] S.S. Kumar, C.S. Kumar, J. Mathiyarasu, K.L. Phani, Stabilized gold nanoparticles by reduction using 3,4-ethylenedioxythiophene-polystyrenesulfonate in aqueous solutions: nanocomposite formation, stability, and application in catalysis, Langmuir 23 (2007) 3401–3408.
[33] P.J. Brown, D.S. Thomas, A. Kohler, J.S. Wilson, J.-S. Kim, C.M. Ramsdale, et al., Effect of interchain interactions on the absorption and emission of poly(3-hexylthiophene), Phys. Rev. B 67 (2003) 064203.
[34] M.C. Gurau, D.M. Delongchamp, B.M. Vogel, E.K. Lin, D.A. Fischer, S. Sambasivan, et al., Measuring molecular order in poly(3-alkylthiophene) thin films with polarizing spectroscopies, Langmuir 23 (2007) 834–842.
[35] L. Li, G. Lu, X. Yang, Improving performance of polymer photovoltaic devices using an annealing-free approach via construction of ordered aggregates in solution, J. Mater. Chem. 18 (2008) 1984–1990.
[36] N. Kiriy, E. Jahne, H.-J. Adler, M. Schneider, A. Kiriy, G. Gorodyska, et al., One-dimensional aggregation of regioregular polyalkylthiophenes, Nano Lett. 3 (2003) 707–712.
[37] Y. Xia, A.G. MacDiarmid, A.J. Epstein, Camphorsulfonic acid fully doped polyaniline emeraldine salt: In situ observation of electronic and conformational changes induced by organic vapors by an ultraviolet/visible/near-infrared spectroscopic method, Macromolecules 27 (1994) 7212–7214.
[38] P. Tehrani, A. Kanciurzewska, X. Crispin, N.D. Robinson, M. Fahlman, M. Berggren, The effect of pH on the electrochemical over-oxidation in PEDOT:PSS films, Solid State Ionics 177 (2001) 3521–3527.
[39] K. Norrman, M.V. Madsen, S.A. Gevorgyan, F.C. Krebs, Degradation patterns in water and oxygen of an inverted polymer solar cell, J. Am. Chem. Soc. 132 (2010) 16883–16892.
[40] G. Volonakis, L. Tsetseris, S. Logothetidis, Impurity-related effects in poly(3-hexylthiophene) crystals, Phys. Chem. Chem. Phys. 16 (2014) 25557–25563.
[41] C.D. Wagner, W.M. Riggs, L.E. Davis, J.F. Moulder, G.E. Muilenberg, Handbook of x-Ray Photoelectron Spectroscopy: A Reference Book of Standard Data for Use in x-Ray Photoelectron Spectroscopy, Perkin-Elmer Corp., Eden Prairie, Minn, 1979.
[42] H. Sirringhaus, P.J. Brown, R.H. Friend, M.M. Nielsen, K. Bechgaard, B.M.W. Langeveld-Voss, et al., Two-dimensional charge transport in self-organized, high-mobility conjugated polymers, Nature 401 (1999) 685–688.
[43] M.J. Panzer, C.D. Frisbie, High carrier density and metallic conductivity in poly(3-hexylthiophene) achieved by electrostatic charge injection, Adv. Funct. Mater. 16 (2006) 1051–1056.
[44] S.S.v. Bavel, M. Barenklau, G.d. With, H. Hoppe, J. Loos, P3HT/PCBM bulk heterojunction solar cells: impact of blend composition and 3D morphology on device performance, Adv. Funct. Mater. 20 (2010) 1458–1463.
[45] J. Huang, S. Virji, B.H. Weiller, R.B. Kaner, Polyaniline nanofibers: facile synthesis and chemical sensors, J. Am. Chem. Soc. 125 (2003) 314–315.
[46] M.H. Dishner, J.C. Hemminger, F.J. Feher, Formation of a self-assembled monolayer by adsorption of thiophene on Au(111) and its photooxidation, Langmuir 12 (1996) 6176–6178.
[47] G. Liu, J.A. Rodriguez, J. Dvorak, J. Hrbek, T. Jirsak, Chemistry of sulfur-containing molecules on Au(111): thiophene, sulfur dioxide, and methanethiol adsorption, Surf. Sci. 505 (2002) 295–307.
[48] M.L. Chabinyc, M.F. Toney, R.J. Kline, I. McCulloch, M. Heeney, X-ray scattering study of thin films of poly(2, 5-bis(3-alkylthiophen-2-yl)thieno[3, 2-b]thiophene), J. Am. Chem. Soc. 129 (2007) 3226–3237.
[49] J.E. Northrup, Atomic and electronic structure of polymer organic semiconductors: p3HT, PQT, and PBTTT, Phys. Rev. B 76 (2007) 245202.
[50] R.J. Kline, M.D. McGehee, M.F. Toney, Highly oriented crystals at the buried interface in polythiophene thin-film transistors, Nat. Mater. 5 (2006) 222–228.

Biographies

Dengke Zhao received his B.S. degree in 2015 from Zhengzhou University of Light Industry and currently he is pursuing his Master degree in organic electronics and electrochemistry in South China University of Technology under the supervision of Prof. Ligui Li. His research interests focus on the design and synthesis of novel functional nanomaterials and their applications in organic electronics, electrochemical energy conversion and storage devices.

Ligui Li completed his bachelor studies at Jilin University (China) in 2004 and received his Ph.D. degree from Changchun Institute of Applied Chemistry (CIAC), Chinese Academy of Sciences (CAS) in January 2010. He then started postdoctoral research in collaboration with Professor Hai-feng Ji at Drexel University in 2010 and Professor Ling Zang at the University of Utah in 2011, respectively. In 2013, he became an associate professor of the College of Environment and Energy at South China University of Technology (SCUT). His recent research interests include organic/polymer opto-electronic materials, preparation of high performance organic/polymer solar cells and perovskite solar cells, and nanomaterials for electrochemical applications.

Wenhan Niu received his Master's degree from Wuhan University of Technology in 2012 and he is pursuing his Ph.D. degree in electrochemistry and novel functional nanomaterials in South China University of Technology. He is interested in organometal halide perovskites solar cells, highly conducting materials for organic electronics and electrochemical applications.

Shaowei Chen finished his undergraduate studies in China in 1991 with a B.Sc. degree in Chemistry from the University of Science and Technology of China, and then went to Cornell University receiving his M.Sc. and Ph.D. degrees in 1993 and 1996, respectively. Following a postdoctoral appointment in the University of North Carolina at Chapel Hill, he started his independent career in Southern Illinois University in 1998. In summer 2004, he moved to the University of California at Santa Cruz and is currently a Professor of Chemistry. He is also an adjunct professor at South China University of Technology. His research interest is primarily in the electron transfer chemistry of nanoparticle materials.